Impacts of Data Assimilation on the Prediction of a Coastal Heavy Rainfall Event during TiMREX (2008) IOP#8

資料同化對 2008 TiMREX IOP#8 沿岸劇烈降水個案的影響

Chuan-Chi Tu[1,4], Yi-Leng Chen[1], Shu-Ya Chen[2], Ying-Hwa Kuo[2,3], and Pay-Liam Lin[4]

涂絹琪 [1,4] 陳宇能 [1] 陳舒雅 [2] 郭英華 [2,3] 林沛練 [4]

[1]**Department of Meteorology, School of Ocean and Earth Science and Technology, University of Hawaii at Manoa**

夏威夷大學氣象系

[2]**University Corporation for Atmospheric Research**

[3] **National Center for Atmospheric Research**

[4]**Institute of Atmospheric Physics, National Central University** 中央大學大氣物理所

Abstract

The impacts of the Constellation Observing System for Meteorology, Ionosphere, and Climate global positioning system (GPS) radio-occultation (RO) soundings and the special data collected during the Terrain-influenced Monsoon Rainfall Experiment (TiMREX) on the numerical weather prediction of a heavy rainfall case during TiMREX (June 16) were investigated. Cycling model runs were employed to assimilate special TiMREX data, global telecommunications system (GTS) data and global positioning system (GPS) Radio Occultation (RO) soundings to improve the model initial conditions provided by the National Centers for Environmental Prediction (NCEP) Global Forecast System (GFS). The GPS RO and special TiMREX soundings have positive impacts on the depiction of subsynoptic flows in the model initial conditions, including the prefrontal moist tongue over the open ocean, the low-level southwesterly monsoon flow, and the weak 500-hPa short-wave trough. The cold pool from the antecedent rains of 14-15 June in the planetary boundary layer with significant orographic blocking over southwestern Taiwan was better resolved in the nested high-resolution domain after the cycling runs with data assimilation as compared with the initial conditions provided by the NCEP GFS. As a result, the local circulations over Taiwan as well as localized heavy rainfall patterns including coastal rainfall along the southwestern coast and afternoon heavy showers in the wake zone over northern Taiwan are better predicted with cycling runs that started 36 hours before the model forecasts.

Keyword: data assimilation, cold pool, orographic blocking, rain evaporative cooling

1. Introduction

Tu et al. (2014) studied a heavy rainfall case over southwestern Taiwan during the TiMREX Intensive Observing Period (IOP)#8 (16 June 2008). On 16 June, heavy rainfall occurred over southwestern Taiwan with a rainfall maximum along the coast (Tu et al. 2014, Fig. 1c and d). The heavy rainfall was associated with a long-lived back-building mesoscale convective system (MCS) upstream of southwestern Taiwan which moved onshore (Xu et al. 2012). The convection developed continuously near the boundary of the warm, moist southwesterly monsoon flow and a cold pool generated by previous rainfall over southwestern Taiwan and the adjacent oceans (Xu et al. 2012; Tu et al. 2014). With the presence of a cold pool, the daytime onshore/upslope flow failed to develop over southwestern Taiwan. As a result, heavy rainfall along the coast continued during the day due to a combination of orographic blocking and the convergence between the offshore wind component and the incoming decelerated flow (Tu et al. 2014). In this study, the cold pool in the boundary layer caused by the antecedent rains is included in the model initial conditions through cycling runs with data assimilation that starts 36 hours before the model forecasts.

2. Data and Methodology

a. Local and satellite observations and YOTC analysis

There were 25 operational conventional surface weather stations, nine rawinsonde stations including special TiMREX sites and four operational Doppler radars over the island of Taiwan during TiMREX. Additionally, soundings launched from the South Ship and the Dong Sha Island provide upstream conditions over the open ocean. Rainfall accumulation maps over the island are generated from 429 rainfall stations, which include conventional surface weather stations and the Automatic Rainfall and Meteorological Telemetry System (ARMTS) (Kerns et al. 2010). The 3-h CMORPH (CPC MORPHing technique) precipitation data with a 0.25° grid were also used (Joyce et al. 2004). The European Centre for Medium-Range Weather Forecasts (ECMWF) Year of Tropical Convection (YOTC) (Moncreff et al. 2012) analysis were used to delineate the subsynoptic weather patterns and moisture tongue. The YOTC gridded data have a 0.5-degree grid interpolated from the original 25-km grid (http://data-portal.ecmwf.int/data/d/yotc_rd).

b. COSMIC global positioning system radio-occultation data and data assimilation

The WRF nested model domains with horizontal grids of 27 km, 9 km, and 3 km are shown in Figure 1a. There are 45 sigma levels[1] from the surface to the 30-hPa level. The Rapid Radiative Transfer Model (RRTM) (Mlawer et al. 1997), Goddard shortwave (Chou and

[1] The full sigma levels are 1.0, 0.995, 0.988, 0.98, 0.97, 0.96, 0.945, 0.93, 0.91, 0.89, 0.87, 0.85, 0.82, 0.79, 0.76, 0.73, 0.69, 0.65, 0.61, 0.57, 0.53, 0.49, 0.45, 0.41, 0.37, 0.34, 0.31, 0.28, 0.26, 0.24, 0.22, 0.2, 0.18, 0.16, 0.14, 0.12, 0.1, 0.082, 0.066, 0.052, 0.04, 0.03, 0.02, 0.01, and 0.000.

Suarez 1994) schemes, Noah land-surface model (LSM) (Chen and Dudhia 2001), and Yonsei University (YSU) planetary boundary layer scheme (Hong et al. 2006) were used. The precipitation process in the model was represented by the grid-resolvable Goddard microphysics (Tao and Simpson 1993) with three classes of ice, including graupel, and the modified Kain-Fritsch cumulus parameterization scheme (Kain 2004). The cumulus parameterization was not applied in the 3-km resolution domain (domain 3). The Central Weather Bureau (CWB) updated land use data were used in the model (Dr. J.-S. Hong, personal communication).

Two experiments are set up to investigate the impact of data assimilation of GPS RO soundings of reflectivity, GTS and TiMREX observations on the initial conditions and model simulations: (1) with assimilation of GPS RO soundings, GTS and TiMREX observations, and available satellite observations (GPSGTS run); and (2) with assimilation of GTS and TiMREX observations and available satellite observations (GTS run). The GTS and satellite observations include SYNOP, METAR, SHIP, BUOY, TEMP, AIREP, PILOT, SATEM, SATOB, and QSCAT. We set up a WRF 3DVAR cycling run for this study. The assimilation experiments are performed with continuous cycling with a ±1.5-h assimilation window. For each cycling experiment, the background (first guess) field is obtained from 6-h WRF forecasts of the previous cycle. The cycling runs starts at 0000 UTC 14 June 2008, ending at 1200 UTC 15 June using the initial and lateral boundary conditions provided by the NCEP FNL data. For the control forecast (CTRL), the initial conditions at 1200 UTC 15 June for all three domains are interpolated from the GFS data with a horizontal resolution of 1^o x 1^o. For all three experiments, the forecast runs start at 1200 UTC 15 June, ending at 0000 UTC 17 June using the lateral boundary conditions provided by the Global Forecast System (GFS) data. The initial conditions and model results from the CTRL run are compared with both cycling runs.

3. Impacts of data assimilation on model initial conditions and subsequent rainfall forecast

a. Subsynoptic scale weather patterns

At 1200 UTC 15 June, a broad moisture tongue extended from the Indo-China Peninsula northeastward to Japan (Fig. 2d). The moisture tongue in GFS forecast extends from southeast coast of China eastward to Taiwan region (Fig. 2c) which is quite different from the YOTC analysis with high moisture content over South China Sea (Fig. 2d). After applying the data assimilation (GPSGTS and GTS cycling runs) to include TiMREX and GTS data with/without GPS data, the moisture tongue is well defined with higher moisture over the South China Sea and lower moisture over the Taiwan Strait (Figs. 2a and b). It is apparent that TiMREX soundings, especially data from the South Ship and the Dong Sha Island have a positive impact in delineating the moisture tongue over the South China Sea. At the 300-hPa level, the domain 1 of GPSGTS run shows a low-pressure center southwest of Taiwan with a short-wave trough extending southwestward (Fig. 3a). In the GTS run, the 300-hPa low/trough extending westward to the southern Taiwan Strait (Fig. 3b) instead of extending southwestward to northern South China Sea as the GPSGTS run (Fig. 3a). On the other hand, for the initial conditions used in the CTRL run, the upper-level low over southwestern Taiwan is not properly resolved as compared with the YOTC analysis (Figs. 3c and d). As will be shown later, the location and orientation of the upper-level low/trough in the initial condition would influence the subsequent forecast of upward motion associated with the low/trough and the rainfall distribution.

b. Cold boundary layer over southwestern Taiwan due to evaporative cooling from antecedent rain

From 0000 UTC 14 June to 1200 UTC 15 June, heavy rainfall occurred over southwestern Taiwan during the passage of a squall line. Both the GPSGTS and the GTS runs underestimate the rainfall amount over southwestern Taiwan during 0000 UTC 14 June - 1200 UTC 15 June (not shown). Nevertheless, comparing the initial condition from the cycling runs and the CTRL run at 1200 UTC 15 June, it is apparent that relatively warm temperatures over southwestern Taiwan and off southwestern Taiwan without cycling runs (Fig. 4e) as compared to the cycling runs (Figs. 4a and c). It is evident that the simulated boundary structure over southwestern Taiwan in the cycle runs is affected by rain evaporative cooling of antecedant rainfall during 0000 UTC 14 June to 1200 UTC 15 June. As a result, without the presence of the cold pool at the model initial time in the CTRL run, the orographic blocking and the turning from southwesterly flow to southerly flow over southwestern Taiwan are less significant (Fig. 4e) as compared with the cycling runs (Figs. 4a and c). From the vertical cross section of potential temperature and winds, we can see that the cold pool below the 800-hPa level only exists in the cycling runs with southerly flow above the surface (Figs. 4b, d and f).

c. Rainfall forecast over southwestern Taiwan

During the daytime of 16 June, heavy rainfall occurs over southwestern Taiwan with a rainfall maximum along the coast (Fig. 5a). The CMORPH rainfall data with a 0.25-degree resolution delineate heavy rainfall systems off the southwestern Taiwan coast as well as over southwestern Taiwan with decreasing rainfall inland (Fig. 20b). However, the CMORPH rainfall data (Fig. 5b) underestimate actual rainfall over land as compared to rain gauge observations (Fig. 5a). Rainfall accumulation from domain 3 in the GPSGTS and the GTS runs over southwestern Taiwan (Figs. 5c and d) is comparable to rain gauge observations with decreasing rainfall inland (Fig. 5a). However, the GPSGTS run shows better rainfall distribution off the southwestern Taiwan coast than the GTS run (Figs. 5c and d) in comparison with the CMORPH rainfall data (Fig. 5b). The GTS run shows a narrow E-W oriented rainband extending too far westward (Fig. 5d) as compared with the CMORPH data (Fig. 5b). This may be because the GPSGTS run has better upper-level low/trough location and orientation in the initial condition for subsequence forecast than the GTS run. The rainfall over southwestern Taiwan and northern South China Sea in the GTS run is slightly overestimated (Fig. 5d) as compared with the rain gauge observations and the CMORPH data (Figs. 5a and b). In general, the GPSGTS shows the best

forecast of the horizontal distribution of rainfall. In the CTRL run, the coastal rainfall is slightly shifted to the north with the offshore rainfall maximum shifted off central western Taiwan (Fig. 5e). The CTRL run significantly underestimates rainfall forecast over southwestern Taiwan and upstream of southwestern Taiwan (Fig. 5e). Another rainfall maximum is simulated in the CTRL run is over the Central Mountain Range (CMR) (Fig. 5e) related to orographic lifting of southwesterly monsoon flow with a westerly wind component. However, the rain gauge observations do not show the 2nd rainfall maximum over the CMR (Fig. 20a). Tu et al. (2014) showed that the orographic lifting of southwesterly monsoon flow is almost absent during the daytime rainfall period as the low-level flow above the surface is parallel to the orientation of the Central Mountain Range. It is apparent that better initial conditions from cycling runs with data assimilation have positive impacts on heavy rainfall prediction.

4. Summary

We selected a heavy rainfall case during the early summer rainy season (16 June 2008) to study how data assimilation of the Terrain-influenced Monsoon Rainfall Experiment (TiMREX) data and global telecommunications system (GTS) data with/without Constellation Observing System for Meteorology, Ionosphere, and Climate (COSMIC) global positioning system (GPS) radio-occultation (RO) soundings would improve the initial conditions for subsequent forecasts of upper-level subsynoptic features, the moisture tongue, local effects and the rainfall distribution.

The GPSGTS and the GTS runs show a better defined moisture tongue with higher total precipitable water (TPW) over the South China Sea at the model initial time (1200 UTC 15 June) than the CTRL run initialized by the GFS data and the YOTC analysis. At the 500-hPa level, the upper-level low/trough west of Taiwan is present in the initial conditions of the GPSGTS and the GTS runs but is not clearly evident in the GFS data.

In addition to improvement in the depiction of the moisture tongue and subsynopitic weather patterns, data assimilation with cycling runs include the rain evaporative cooling from the antecedent rains during 14-15 June 2008 and local effects in the initial conditions of the nested domains. With cycling runs, the air temperature in the boundary layer over southwestern Taiwan in the initial condition is relatively cold with significant orographic blocking in agreement with observations (Tu et al. 2014). Above the cold pool, the southwesterly monsoon flow turns to southerly flow over southwestern Taiwan. In contrast, in the CTRL run, the air in the boundary layer over southwestern Taiwan is relatively warm and the southwesterly flow has a westerly wind component impinging on the Central Mountain Range in the model initial conditions. With westerly wind component and the development of daytime upslope flow in the CTRL run, a rainfall maximum in the mountainous interior due to orographic lifting is predicted. However, in the GPSGTS and the GTS runs, only coastal rainfall is predicted over the convergence zone over southwestern Taiwan between the decelerating incoming flow and the offsher flow component along the coast in agreement with observations.

References

Chen, F., and J. Dudhia, 2001: "Coupling an advanced land-surface/ hydrology model with the Penn State/ NCAR MM5 modeling system. Part I: Model description and implementation", Mon. Wea. Rev., 129, 569–585.

Chou, M.-D., and M. J. Suarez, 1994: An efficient thermal infrared radiation parameterization for use in general circulation models. NASA Tech. Memo. 104606, 3, 85 pp

Hong, S.-Y., and Y. Noh, and J. Dudhia, 2006: "A new vertical diffusion package with an explicit treatment of entrainment processes", Mon. Wea. Rev., 134, 2318–2341.

Joyce, R.J., J.E. Janowiak, P.A. Arkin, and P. Xie, 2004: CMORPH: A Method That Produces Global Precipitation Estimates From Data At High Spatial And Temporal Resolution. *J. Hydrometeor*, **5**, 487-503.

Kain, J. S., 2004: "The Kain-Fritsch convective parameterization: An update", J. Appl. Meteor., 43, 170–181.

Kerns, B., Y.-L. Chen, and M.-Y. Chang, 2010: The diurnal cycle of winds, rain and clouds over Taiwan during the Mei-Yu, summer, and autumn regimes. *Mon. Wea. Rev.* **138**, 497–516.

Mlawer, E. J., S. J. Taubman, P. D. Brown, M. J. Iacono, and S. A. Clough, 1997: "Radiative transfer for inhomogeneous atmosphere: RRTM, a validated correlated-k model for the long- wave", J. Geophys. Res., 102 (D14), 16663–16682.

Moncrieff, M. W., D. E. Waliser, M. J. Miller, M. A. Shapiro, G. R. Asrar, and J. Caughey, 2012: "Multiscale convective organization and the YOTC virtual global field campaign", Bull. Amer. Meteor. Soc., 93, 1171–1187.

Tao, W.-K., and J. Simpson, 1993: "The Goddard cumulus ensemble model. Part I: Model description", Terr. Atmos. Oceanic Sci., 4, 35–72.

Tu, C.-C., Y.-L. Chen, C.-S. Chen, P.-L. Lin and P.-H. Lin, 2014: "A comparison of two heavy rainfall events during the Terrain-influenced Monsoon Rainfall Experiment (TiMREX) 2008", Mon. Wea. Rev., 142, 2436-2463.

Xu, W., E. J. Zipser, Y.-L. Chen, C. Liu, Y.-C. Liou, W.-C. Lee, and B. J.-D. Jou, 2012: "An orography-associated extreme rainfall event during TiMREX: initiation, storm evolution, and maintenance", Mon. Wea. Rev., 140, 2555–2574.

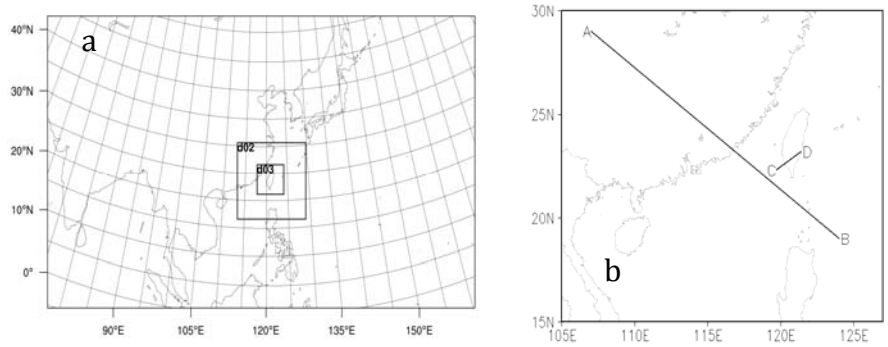

Fig. 1 (a) The three domains of the WRF model simulation with horizontal grid sizes of 27 km, 9 km, and 3 km, respectively. (b) Cross section lines AB and CD.

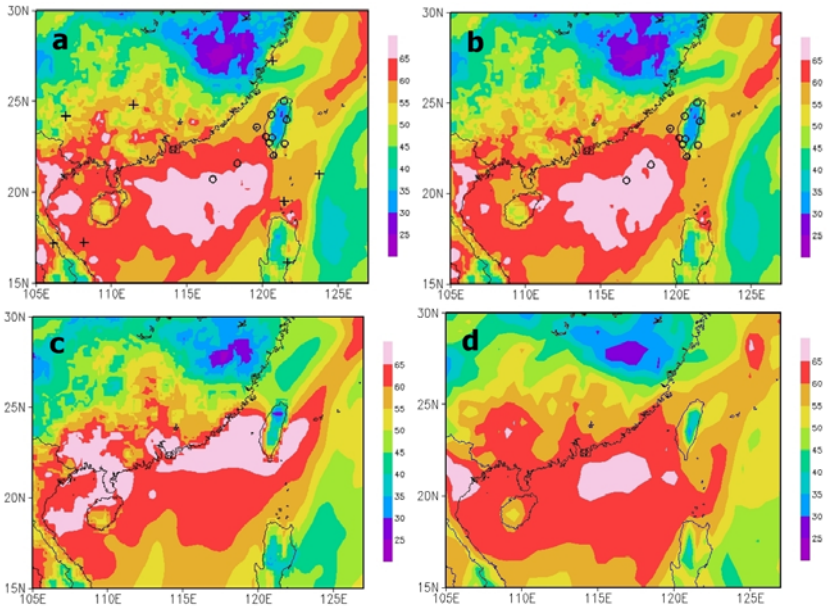

Fig. 2. TPW at 1200 UTC 15 June from the domain one: (a) GPSGTS run, (b) GTS run, (c) GFS forecast, and (d) YOTC analysis.

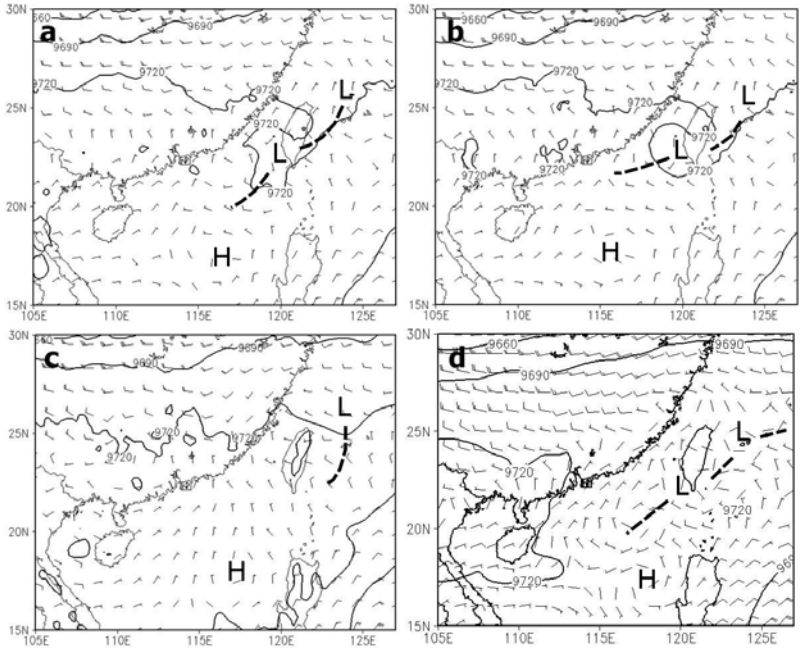

Fig. 3. (a) 300-hPa geopotential height (gpm) and winds (m s^{-1}, full barb represents 10 m s^{-1}) at 1200 UTC 15 June from the GPSGTS run, (b) GTS run, (c) CTRL run, and (d) YOTC analysis.

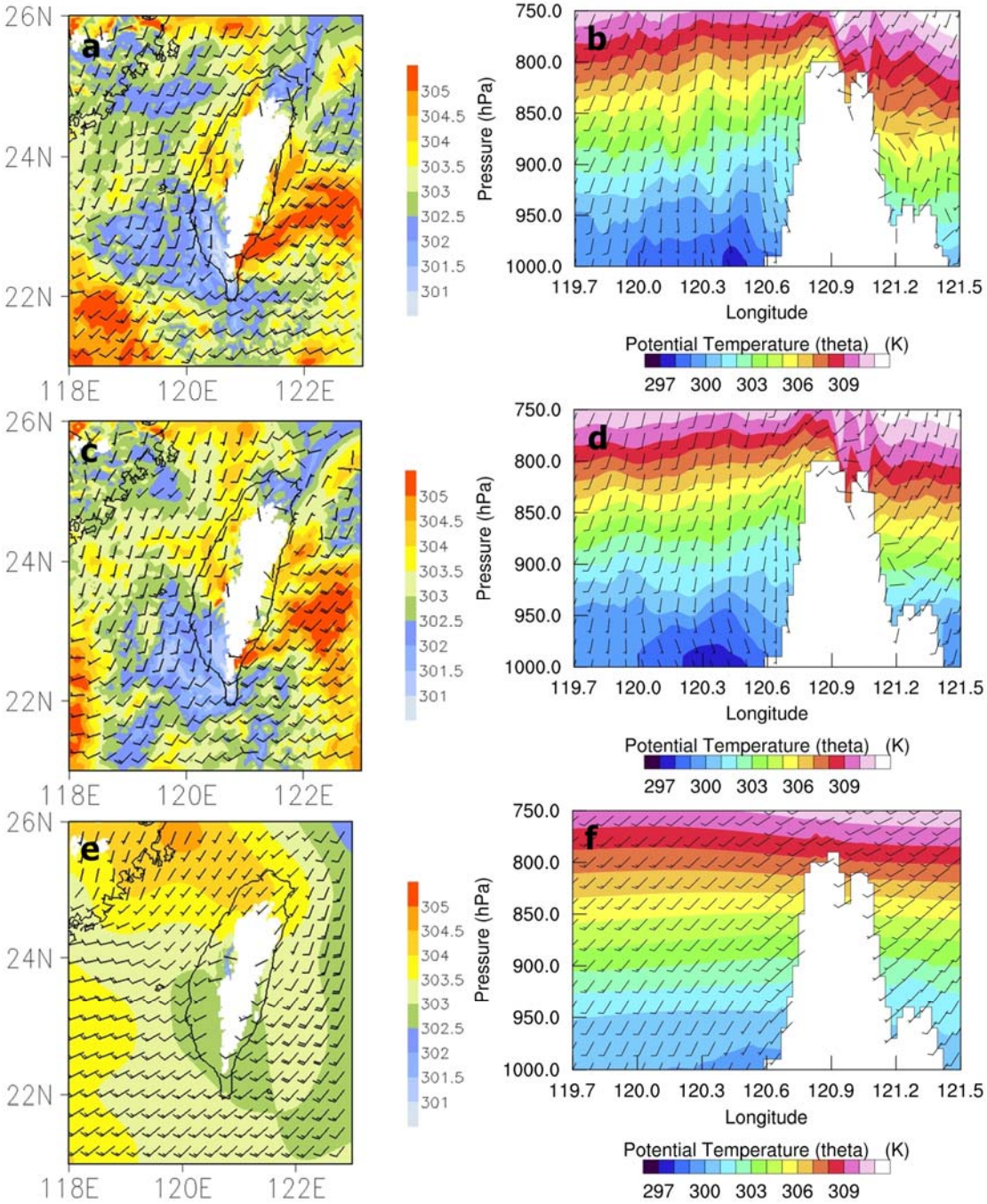

Fig. 4. (a) The 900-hPa potential temperature (K) and winds (m s^{-1}, full barb represents 10 m s^{-1}) and (b) the cross section of potential temperature (K) and winds (full barb represents 10 m s^{-1}) along the line CD in Figure 1 at 1200 UTC 15 June for domain 3 in the GPSGTS run. (c) and (d) Same as (a) and (b), but for the GTS run. (e) and (f) Same as (a) and (b), but for the CTRL run.

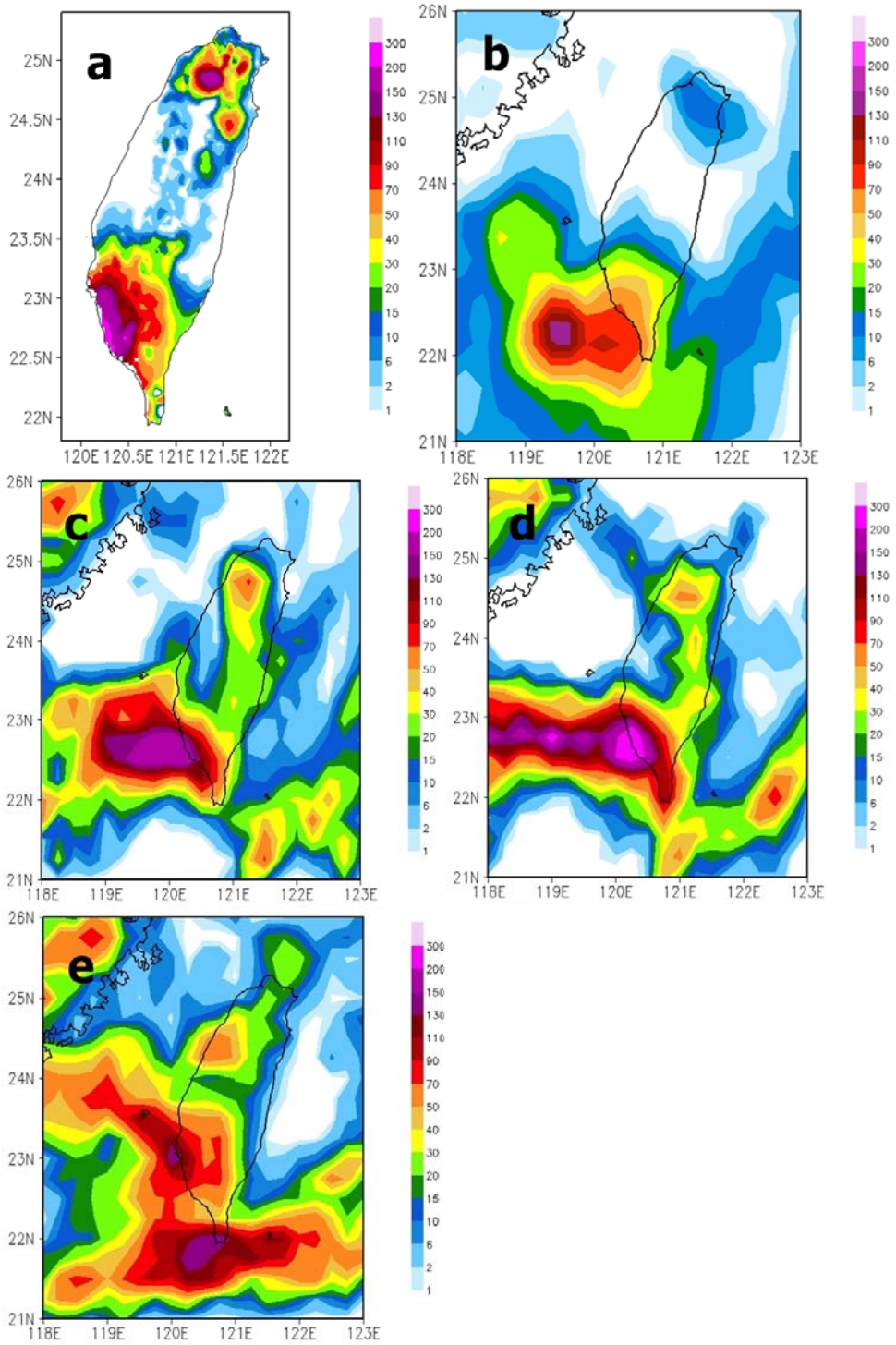

Fig.5 The rainfall accumulation during 0000-1200 UTC 16 June from (a) rain gauge observations, (b) CMORPH data, (c) GPSGTS run, (d) GTS run, and (e) CTRL run (interpolation from Domain 3 results).